

^{30}S RI Beam Production & XRBs

D. Kahl^a, A. A. Chen^a, D. N. Binh^b, J. Chen^a, T. Hashimoto^b, S. Hayakawa^b,
A. Kim^c, S. Kubono^b, Y. Kurihara^b, N. H. Lee^c, S. Michimasa^b, S. Nishimura^d,
C. V. Ouellet^a, K. Setoodehnia^a, Y. Wakabayashi^b, and H. Yamaguchi^b.

^aDepartment of Physics & Astronomy, McMaster University (Canada)

^bCenter for Nuclear Study, Graduate School of Science, University of Tokyo (Japan)

^cDepartment of Physics, Ewha Womans University (Korea)

^dRIKEN (The Institute of Physical and Chemical Research) (Japan)

Astrophysical Motivation

The $^{30}\text{S}(\alpha,p)^{33}\text{Cl}$ reaction is a significant link in the αp -process, which competes with the rp -process on accreting neutron stars¹, but there is no experimental data to date.

- X-Ray Bursts (XRBs) with multiple peaks in their bolometric luminosity are explained by Fisker, Thielemann & Wiescher as multiple releases of nuclear energy, separated by a nuclear waiting point.²
- Low mass accreting neutron star binary systems
 - Assume accretion at 8×10^{-10} solar masses / year
- Accreted material assumed to be of solar composition³
 - 90.99% H, 8.87% He, 0.03% C, 0.01% N, 0.08% O
- β -limited hot CNO cycle pre-burst ($T_0 = 0.1 - 0.2$ K)
- Thermal instabilities \rightarrow explosive nucleosynthesis
 - hot CNO breakout \rightarrow ^{19}Ne and ^{21}Na seed nuclei
 - rp -process ($T_0 = 0.4 - 1.2$ K)
- Recurrent bursts, ~ 100 known XRBs
- 4 observed bolometrically multi-peaked bursts^{4,5,6,7}
 - These constrain XRB models
 - Many proposed explanations
- Fisker *et al.* propose nuclear waiting point
 - Infer bottleneck at ^{30}S
 - β^- -decay on order of burst rise-times
 - Burning inhibited by photodisintegration
- Varying the theoretical reaction rate of $^{30}\text{S}(\alpha,p)^{33}\text{Cl}$ by a factor of 100, Fisker *et al.* produce a different burst profile where the double peak structure is notably diminished.
- We will perform a direct experimental measurement of the $\alpha(^{30}\text{S},p)^{33}\text{Cl}$ cross section
 - To do this, we need a low energy ^{30}S RI beam of high intensity ($\sim 10^5$ pps) and purity

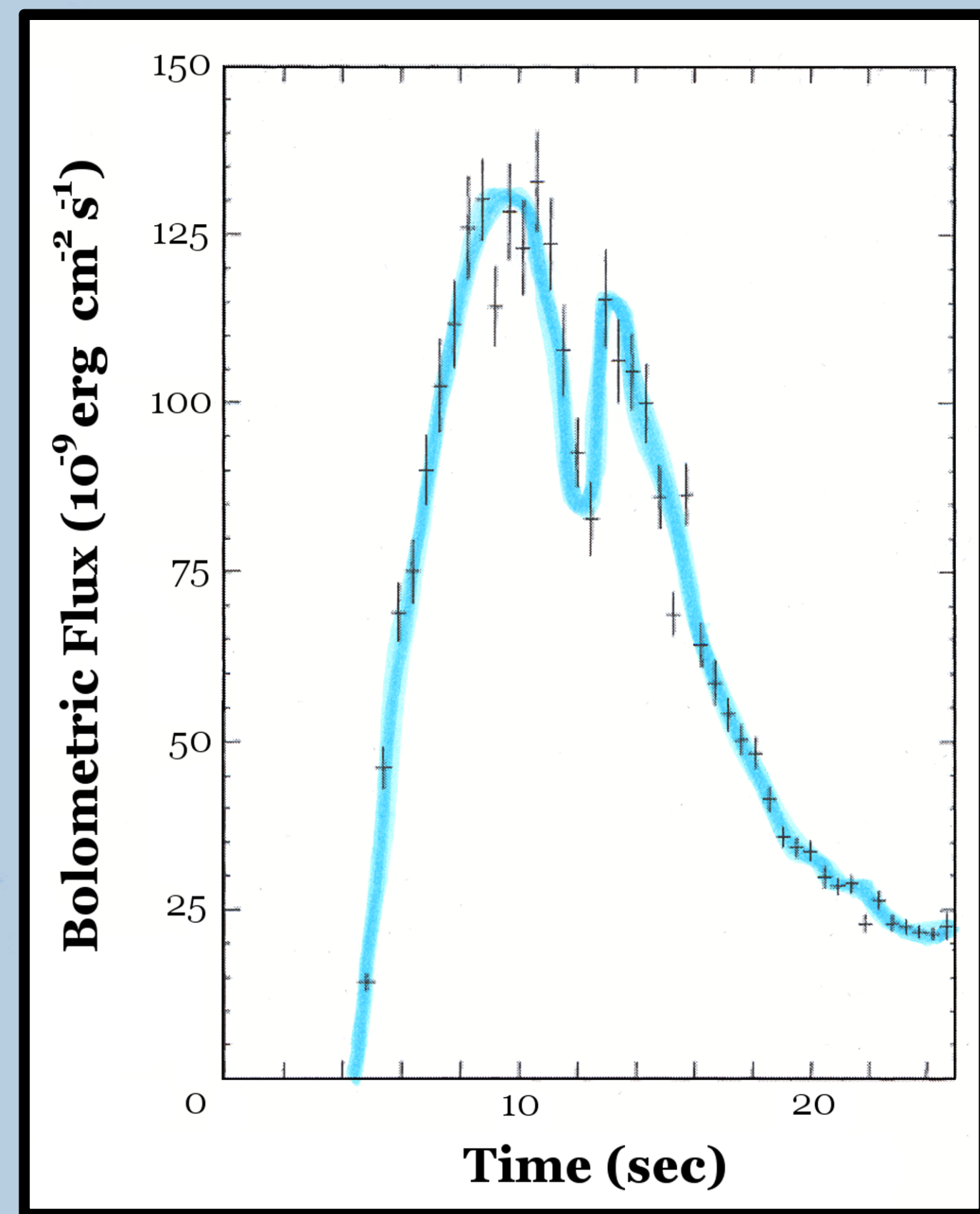


Figure 1: Double-peaked XRB 4U 1608-52 spectrum, plotted as time versus bolometric flux (10^{-9} in cgs). Notice 25% decrease in luminosity after first peak.⁷ Blue line is strictly a visual guide, not a fit to the data.

Planned Experimental Setup

To measure $\alpha(^{30}\text{S},p)^{33}\text{Cl}$ cross section, we will bombard a thick ^4He gas cell with a mono-energetic beam of ^{30}S . We will gate on ^{30}S beam ions in RF and ToF and detect reaction protons downstream.¹¹

- Scan Gamow window for $T_0 = 1.2 - 2.0$ K $\rightarrow E_{\text{beam}} = 13.4 - 32.3$ MeV on target
- Use extended (150 mm depth), havar windowed (2.5 μm foil), thick ^4He gas target
 - ^4He pressure of ~ 200 Torr is needed to scan this energy range
 - Target includes windows perpendicular to beam axis to detect recoil protons up to $\theta = 90^\circ$
- Reconstruct event-by-event $\alpha(^{30}\text{S},p)$ reactions
 - Incident beam ions tracked with 2 delay-line PPACs¹² or Multi-Channel Plates (MCPs)
 - Gate on beam ions with correct RF and Time of Flight (ToF)
 - RF is cyclotron radiofrequency, which starts the clock for flight time between F0 and F3
 - ToF is the flight time between the F3 PPACs
 - Recoil protons detected with three or four ΔE -E silicon telescopes at different angles
 - NaI detectors to measure γ -rays
- Experimental setup and detection efficiency tested in July 2008 via $\alpha(^{28}\text{Si},p)^{29}\text{Al}$ ^{13,14,15}
- $\alpha(^{30}\text{S},p)$ measurement planned for 2009.

Results

All our ^{30}S RI beam results were improved with use of $^{28}\text{Si}^{10+}$ (7.54 MeV/u) primary beam. $^{30}\text{S}^{16+}$ achieved 30% purity, 30 MeV, and 500 pps per 10 pA at F3. $^{30}\text{S}^{14+}$ achieved 0.8% purity, 32 MeV, and 1.2×10^4 pps per 10 pA at F3.¹⁶

- PSD is position sensitive detector
 - 69 μm thick silicon
 - Fully stops these ions
 - 16 x 16 channels
- All data here include use of WF
 - Increases RI beam purity
- Figure 4 shows leaky primary beam in the $^{30}\text{S}^{15+}$ RF v. E plot
 - RF v. ToF gate applied
 - $\alpha(^{28}\text{Si},p)$ indistinguishable from $\alpha(^{30}\text{S},p)$ in this case
 - Cannot be used for $\alpha(^{30}\text{S},p)$
- Dipoles separate on p/q ratio
 - $^{28}\text{Si}^{14+}$ & $^{30}\text{S}^{15+}$ have same A/q
 - Very hard to isolate $^{30}\text{S}^{15+}$
- Need 10^5 pps to measure $\alpha(^{30}\text{S},p)$
- Figure 5 shows $^{30}\text{S}^{16+}$ is easy to distinguish
 - Max 500 pps per 10 pA
 - Intensity too low
 - 80% WF transmission
- Figure 6 shows we separate $^{30}\text{S}^{14+}$ in RF v. ToF spectrum
 - $\sim 1 \times 10^4$ pps per 10 pA
 - Very little time to tune CRIB
 - 24% WF transmission
 - No degrader used at F1
- F1 degrader did not help much
 - Decrease intensity by 20%
 - 64% WF transmission
 - Same purity on target

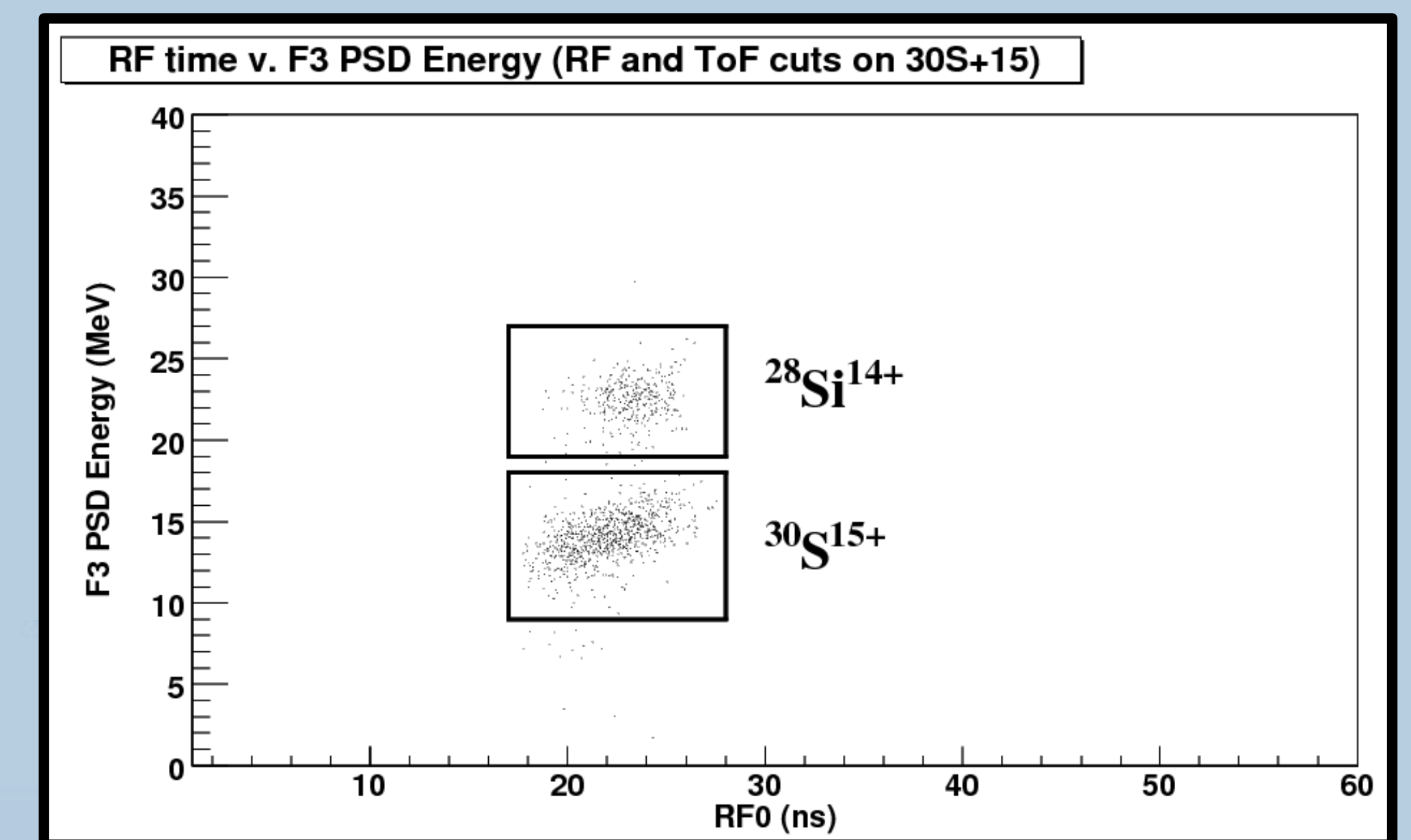


Figure 4: December 2006 run showing beam RF time versus energy at F3. 813 counts of $^{30}\text{S}^{15+}$, 335 counts of $^{28}\text{Si}^{14+}$.

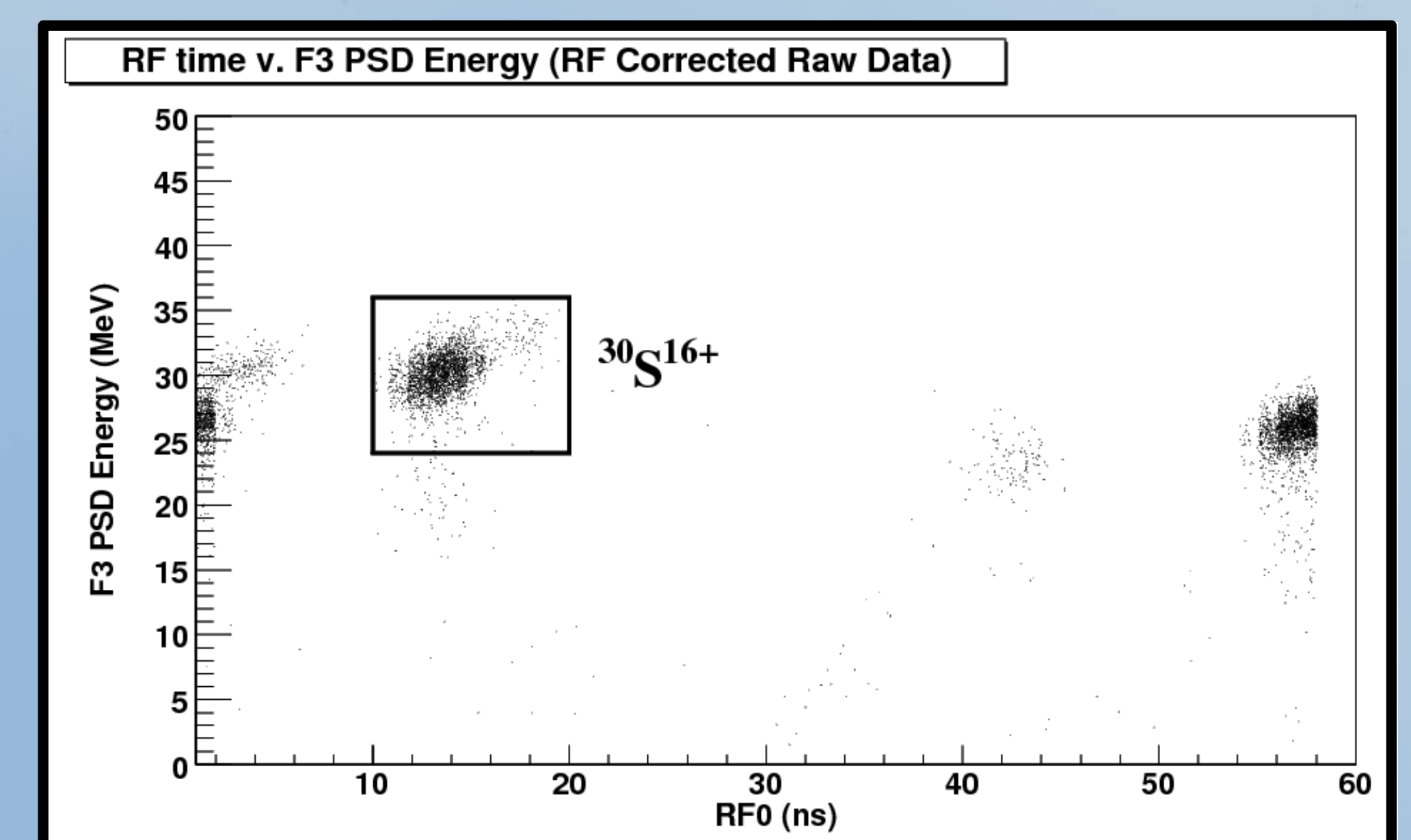


Figure 5: May 2008 run showing beam RF time versus energy at F3. $^{30}\text{S}^{16+}$ comprises 30% of the data.

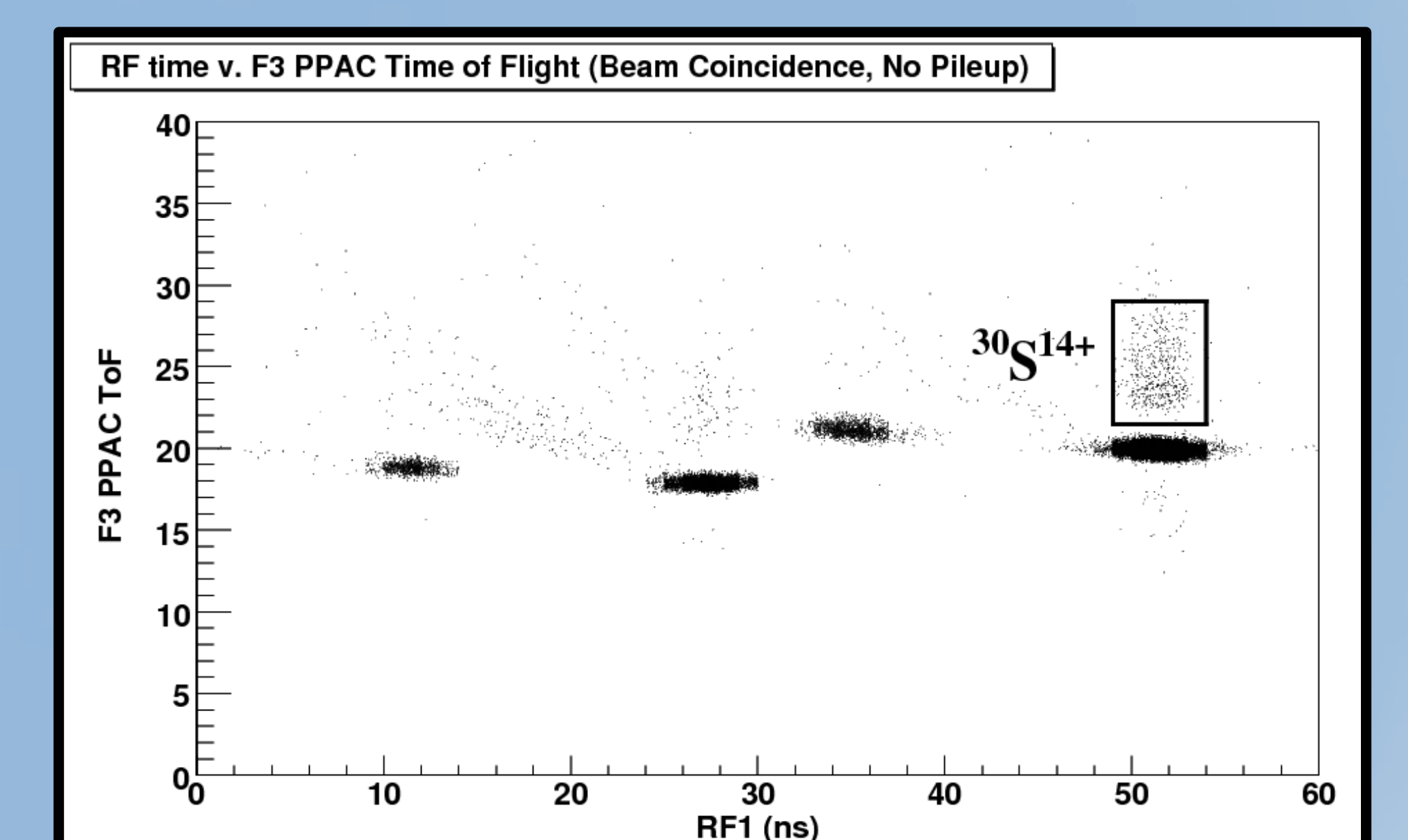


Figure 6: May 2008 run showing beam RF time versus ToF at F3. $^{30}\text{S}^{14+}$ comprises 0.8% of the data.

Future

- AVF Cyclotron improvements
 - > 8 MeV/u $^{28}\text{Si}^{10+}$ at 30 pA
- Expect we can get ^{30}S at 10^5 pps
 - Separated $^{30}\text{S}^{14+}$ at 10^4 pps
 - Cyclotron improvements help
 - Test up to 450 Torr ^3He at F0
 - Optimize CRIB for $^{30}\text{S}^{14+}$
 - May tune slit positions to improve purity
 - Mean charge-states: $^{30}\text{S}^{12+,13+}$
 - Tested charge-state booster in July 2008

References and Works Cited

- [1] H. Schatz, *et al.*, *ApJ* **524** (1999) 1014.
- [2] J. L. Fisker, F.-K. Thielemann, & M. Wiescher, *ApJ* **608** (2004) L61.
- [3] E. Anders & M. Grevesse, *Geochim. Cosmochim. Acta* **53** (1989) 197.
- [4] E. Kuuikers *et al.*, *A&A* **382** (2002) 947
- [5] M. Sztajno *et al.*, *ApJ* **299** (1985) 487.
- [6] J. van Paradijs *et al.*, *MNRAS* **221** (1986) 617.
- [7] W. Penninx *et al.*, *A&A* **208** (1989) 146.
- [8] W. Bohné *et al.*, *Nucl. Phys. A* **378** (1982) 525.
- [9] S. Kubono *et al.*, *Eur. Phys. J. A* **13** (2002) 217.
- [10] Y. Yanagisawa *et al.*, *Nuc. Inst. and Meth. A* **539** (2005) 74.
- [11] W. Bradfield-Smith *et al.*, *Nuc. Inst. and Meth. A* **425** (1999) 1.
- [12] H. Kumagai *et al.*, *Nuc. Inst. and Meth. A* **470** (2001) 562.
- [13] M. A. Buckley & J. D. King, *Can. J. Phys.* **62** (1984) 134.
- [14] K.-M. Källman *et al.*, *Eur. Phys. J. A* **16** (2003) 159.
- [15] J. G. Ross *et al.*, *Phys. Rev. C* **52** (1995) 1681.
- [16] D. Kahl *et al.*, *CNS Annual Report 2006 CNS-REP-76* (2007) 1.

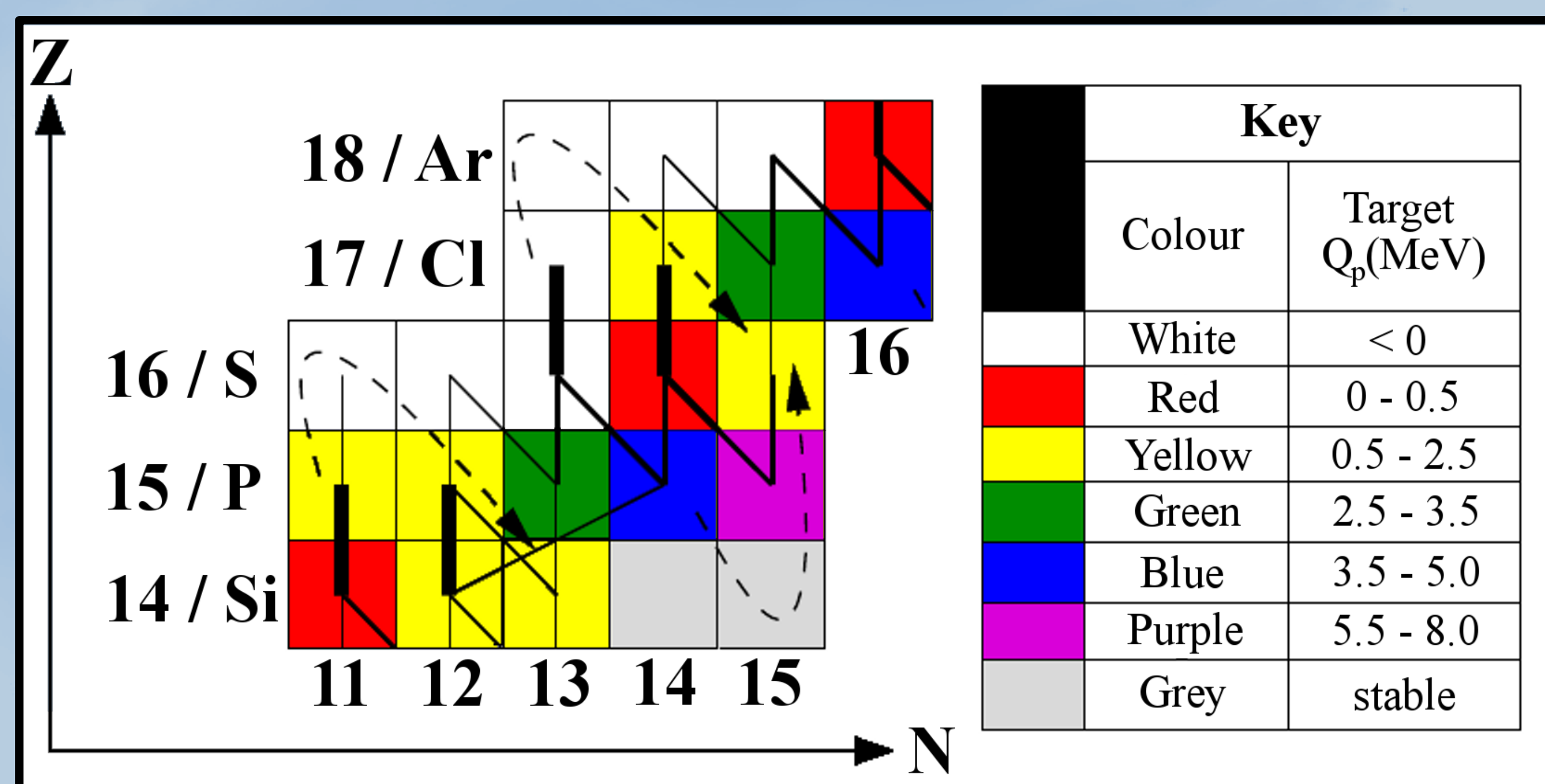


Figure 2: N vs. Z diagram near ^{30}S ($Z=16$, $N=14$). Colour indicates energy released during proton capture (Q_p). Black lines indicate strength of the reaction path for (p,γ) , β^+ , and (α,p) , except for thick vertical lines indicating $(p,\gamma)-(\gamma,p)$ equilibrium. XRB nucleosynthesis must pass through ^{30}S ($t_{1/2}=1.178$ s). $^{30}\text{S}(\alpha,p)$ not shown – no experimental data.²

^{30}S RI Beam Development

We successfully separated out the proton-rich isotope ^{30}S , after bombarding a cryogenic ^3He gas cell with a stable ^{28}Si beam using the $^3\text{He}(^{28}\text{Si},n)^{30}\text{S}$ reaction.⁸

- Work performed at CRIB facility^{9,10}
 - CNS radioactive ion beam separator
 - CRIB is operated by the University of Tokyo and located at RIKEN
- Two ^{30}S beam development runs
 - Two days in December 2006
 - Two days in May 2008
- Tested two primary beam conditions
 - $^{28}\text{Si}^{9+}$ (6.9 MeV/u and 100 pA)
 - $^{28}\text{Si}^{10+}$ (7.54 MeV/u and 10 pA)
- Production target is ^3He gas
 - Cooled to 80K with LN_2
 - Confined with 2.2 μm havar foils
 - Tested pressures 200, 300, 400 Torr
- Particle identification at F2
 - Obtain position and timing of reaction products by inserting a parallel plate avalanche counter (PPAC) at F2
 - Obtain energy of reaction product by inserting a 1.5 mm thick silicon strip detector (SSD)
- Tested a 1.5 μm thick aluminized mylar degrader at F1 to increase charge-state separation
- Increase purity at F3 by using a Wien filter to select a specific particle velocity
- Adjustable slits are located at each focal plane to tune CRIB acceptance
- ^{28}Si beam extracted from Hyper ECR ion source (14 GHz) and accelerated by RIKEN AVF cyclotron

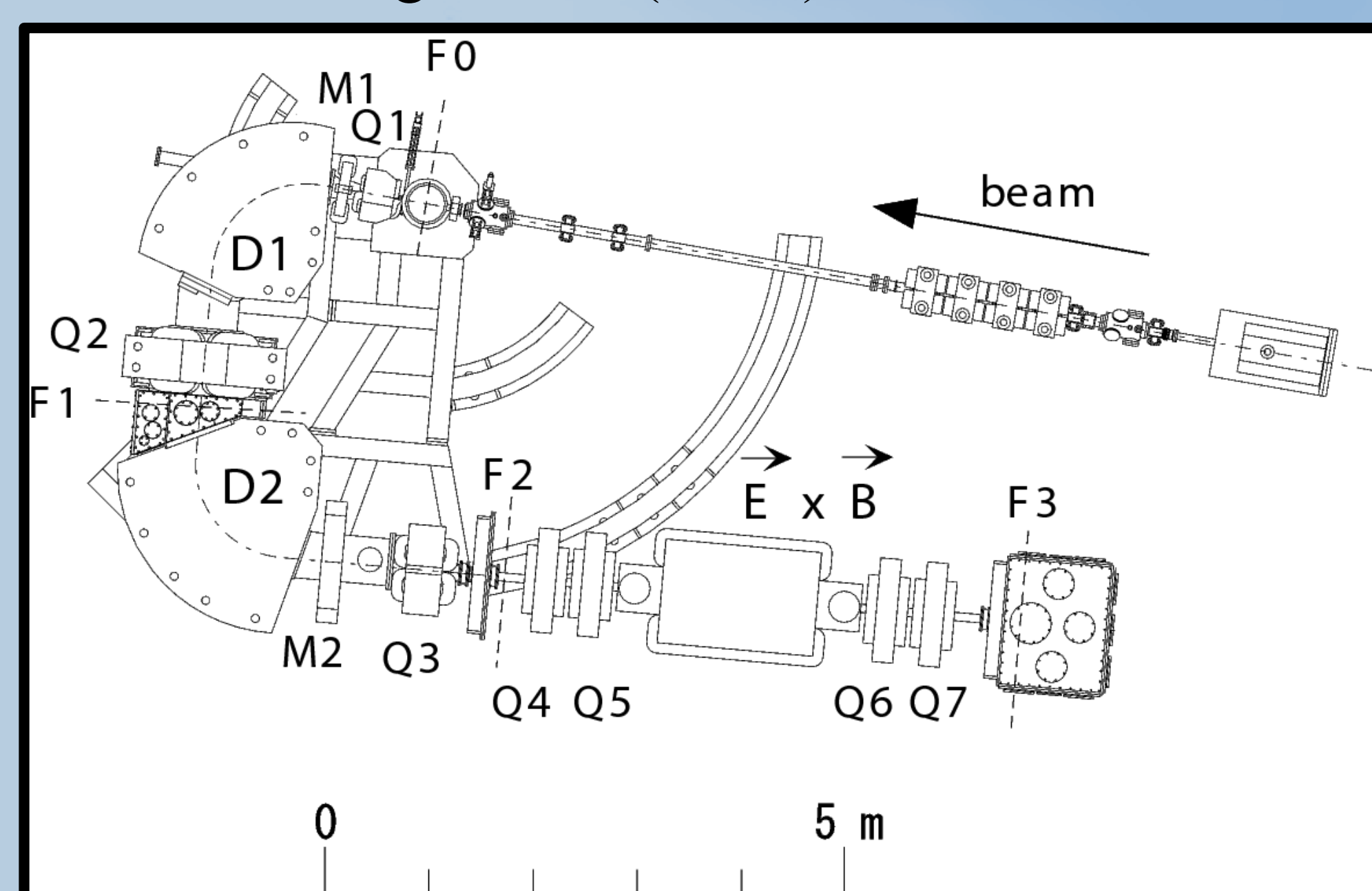


Figure 3: CRIB separator schematic. The primary beam enters from the upper right side and impinges a cryogenic, windowed gas target at F0. F1 is the momentum dispersive focal plane. F2 is a doubly achromatic focal plane. F3 is the experimental scattering chamber. D1 & D2 are magnetic dipoles. Q1-Q7 are magnetic quadrupoles. M1 & M2 are magnetic multipole. E x B is the Wien filter (WF).